
ALGORITHMIC NAVIGATION REDUCES ROUTE DIVERSITY AND AMPLIFIES EMISSIONS INEQUALITY IN CITIES

Giuliano Cornacchia

ISTI-CNR, Pisa, Italy

Department of Computer Science, Pisa, Italy

giuliano.cornacchia@isti.cnr.it

Mirco Nanni

ISTI-CNR, Pisa, Italy

mirco.nanni@isti.cnr.it

Dino Pedreschi

Department of Computer Science, Pisa, Italy

dino.pedreschi@unipi.it

Luca Pappalardo

ISTI-CNR, Pisa, Italy

Scuola Normale Superiore, Pisa, Italy

luca.pappalardo@isti.cnr.it

ABSTRACT

The collective impact of GPS navigation services is unclear: while beneficial to the user, they can also cause chaos if too many vehicles are driven through the same few roads. Our study employs a simulation-based framework for evaluating the impact of navigation services, integrating real-world mobility data and route recommendations offered by leading navigation services' APIs. The results demonstrate a universal pattern of amplified conformity: increasing adoption rates of navigation services cause a reduction of route diversity of mobile travellers and increased concentration of traffic and emissions on fewer roads, thus exacerbating an unequal distribution of negative externalities on selected neighbourhoods. Although navigation services recommendations can help reduce CO2 emissions when their adoption rate is low, these benefits diminish or even disappear when the adoption rate is high and exceeds a certain city- and service-dependent threshold. We summarize these discoveries in a non-linear function that connects the marginal increase of conformity with the marginal reduction in CO2 emissions. To isolate the core dynamics of traffic and emissions concentration, we replicate our experiments in simplified mobility settings, confirming that these patterns emerge independently of real-world urban complexity. Our simulation approach addresses the challenges posed by the complexity of transportation systems and the lack of data and algorithmic transparency.

Introduction

The ascent of human-AI ecosystems in which humans interact with various forms of algorithms, including AI assistants and recommender systems, multiplies the possibility for the emergence of large-scale behaviour patterns, possibly with unintended consequences [1, 2, 3, 4, 5]. The aggregation of many individually “good” recommendations may have unintended outcomes because human choices, influenced by these recommendations, interfere with each other on top of shared resources.

We have evidence of this phenomenon in various contexts [1, 3]. Personalised recommendations on social media help users deal with information overload but may artificially amplify echo chambers, filter bubbles, and processes of radicalisation [6, 7, 8, 9, 10, 11, 12]. Profiling and targeted advertising may further increase inequality and monopolies, with the harms of perpetuating and amplifying biases, discriminations, and the “tragedy of the commons” [13, 14, 15]. Mobile applications providing pedestrians directions to avoid high-crime areas make users feel safer but may make dangerous areas more isolated, thus favouring a further increase in crime [16, 17, 18].

Notwithstanding, the collective impact of other pervasive recommender systems is still little understood. A notable example is commercial navigation services (e.g., TomTom, Google Maps). These services recommend routes to a destination, considering traffic conditions. Despite their indubitable usefulness, especially when exploring an unfamiliar city, navigation services may also create chaos if too many drivers are directed on a few roads [19, 20, 21]. This was the case of Leonia, a small town in New Jersey, USA. In 2017, GPS navigation apps repeatedly rerouted drivers on congested highways through Leonia’s narrow streets, creating such congestion that people could not get out of their driveways [21, 20]. Seven years later, in October 2024, a similar scenario played out in an Italian mountain area: many travellers, trying to bypass highway queues by following Google Maps’ suggestions, were stuck in severe traffic jams snaking through local villages [22]. These are not isolated cases: increasingly, many towns globally have been grappling with the local gridlock caused by well-intentioned navigation apps [23, 24].

These incidents are extreme by-products of a generalised phenomenon: the impact of AI-driven recommender systems on urban traffic. Research in this domain yields fragmented and contradictory results, primarily focused on specific navigation services and individual urban contexts [1, 4, 3, 25, 26]. A notable exception is a 2021 study – unfortunately not replicable – conducted by Google Maps in Salt Lake City, providing valuable insights into the real-world effects of algorithmic navigation on human mobility [26]. The study identified measurable benefits, including an average reduction of 6.5% in travel time and a 1.7% decrease in CO₂ emissions. Apart from this particular study, existing literature primarily examines routing principles rather than commercial navigation services. These studies suggest routing strategies can effectively mitigate CO₂ and NO_x emissions [27, 28, 29, 30], reduce energy consumption [27], decrease fuel usage [28], lower vehicle miles travelled [31], and minimize accident risks [32]. Nevertheless, they also highlight potential drawbacks, such as increased travel times, heightened exposure of populations to NO_x, elevated traffic volumes in certain areas [29, 30], and unintended redistribution of highway traffic onto local streets, parks, tourist destinations, and slower roads [31, 32]. Overall, we lack robust methodologies to fully understand the multifaceted impact of navigation services on some externalities, such as road network usage and CO₂ emissions. For example, what would the urban impacts of various navigation services be under different traffic conditions and adoption rates? This article contributes to this intriguing debate.

We design a data-informed simulation framework to study the influence of navigation services on road network usage and CO₂ emissions. Our open-source framework is a realistic digital twin of urban traffic that receives inputs from real-world mobility data and integrates the route recommendations offered by commercial navigation services’ APIs. We use the framework to conduct controlled simulations in three cities, in which we vary the adoption rate of a navigation service. For each adoption rate, vehicles are randomly divided into treatment and control groups, with the treatment group following route recommendations and the control group not adhering to them.

We find that the aggregate impact of route recommendations is far from negligible. First, at high adoption rates and across all cities and navigation services, route diversity considerably decreases, i.e., vehicles are predominantly routed through fewer roads. These roads are typically highways and major arterial corridors, where CO₂ concentrations are further intensified. Second, we focus on the relationship between adoption rate and CO₂ emissions. We discover that at low traffic loads – when a few vehicles traverse the city (e.g., off-peak hours) – navigation services consistently suggest optimal routes through an almost-empty road network, thereby reducing CO₂ emissions. However, at high traffic loads – when the traffic on the road network approaches congestion (e.g., peak hours) – the impact of navigation services depends on the adoption rate. At a low adoption rate, the impact of navigation services is mainly beneficial and CO₂ emissions decrease. However, once the penetration rate exceeds a service-specific threshold, these benefits diminish, disappear, or even reverse. The relationship between the marginal shift in route diversity and the marginal shift of CO₂ emissions is well described by an exponential function. This enables us to forecast the marginal change in CO₂ emissions as route diversity decreases, given the expansion of navigation service adoption throughout the population. To uncover the mechanisms underlying the relationship between service adoption and urban traffic, we replicate our experiments on a simplified representation of mobility demand and road networks. We then analyse how route diversity and CO₂ emissions vary across different adoption rates, finding that our results closely match the results obtained for real cities.

Our study provides an unprecedented view of the impact of navigation services on urban traffic concerning the services’ adoption rate. Our framework, which applies to any city provided the availability of mobility demand and road network data, may provide practical support for decision-makers in managing and mitigating the urban impact of digital platforms. This becomes especially pertinent within the context of emerging regulations such as the European Union’s Digital Services Act [33], which mandates risk assessments for major digital platforms and advocates for closer examination of their societal effects.

Simulation framework

We design a simulation framework to study how various navigation services affect urban traffic under various adoption rates and traffic loads. This framework exploits SUMO, an open-source, state-of-the-art simulation tool that generates a lifelike representation of urban traffic based on a given road network and mobility demand (see Methods for details) [34]. The simulation can capture the behaviour of a set of vehicles, including their routes, traffic congestion, queues at traffic lights, and slowdowns due to heavy traffic, providing a realistic digital twin of vehicular traffic.

A city’s road network can be represented as a directed graph, where the set of nodes represents road intersections and the set of edges represents road edges (individual segments that connect road intersections). We use road networks made available on the public geographic information system OpenStreetMap (see Methods for details). We describe the mobility demand within the city as an origin-destination (OD) matrix M , where each element $m_{o,d} \in M$ indicates the number of trips that start from location o and end at location d . An OD matrix may be obtained in various ways, such as through travel surveys, GPS traces, mobile phone records, or smart card transactions [35, 36, 37, 38]. In this study, we divide the city into equally sized square tiles and leverage real-world GPS traces from thousands of private vehicles to compute the number of vehicles moving between any two tiles (see Methods for details). We then randomly select N trips, where each trip $T_v = (e_o, e_d, t)$ is obtained by randomly selecting an element $m_{o,d} \in M$ with probability $p_{o,d} \propto m_{o,d}$, uniformly selecting two road edges e_o, e_d within the corresponding tiles o and d , and uniformly selecting a starting time t during one hour. This procedure constitutes a foundational step of the simulation framework, translating the aggregate mobility captured by the OD matrix into a set of individual vehicle trips. This conversion enables the simulation of realistic traffic dynamics that reflect the underlying spatial pattern of urban mobility demand. See Supplementary Note 1 for further details on the computation of the mobility demand.

We rely on public API-based navigation services to generate trip routes on the road network (see Methods for details). These services recommend a route between an origin road edge e_o and a destination road edge e_d considering various

factors, such as the typical traffic conditions at the time t when the trip (e_o, e_d, t) starts. The trip (e_o, e_d, t) allows us to simulate drivers’ typical requests for these services, such as “Take me from location A to location B by car at 3:30 PM”. Note that navigation services also consider real-time traffic conditions in the real world when providing routes. These real-world conditions can be unpredictable due to exogenous factors that happen in real time (e.g., strikes, accidents, and works in progress). To ensure consistency with our simulated traffic, we force the use of historical information by making the request for a future time with respect to the time of the simulation. This means the suggested route is the most convenient choice (according to the navigation service) given the city’s typical traffic conditions at that time.

We consider a collection S of popular navigation services with public APIs, including Google Maps (GM), MapBox (MB), Bing Maps (Bi), TomTom fastest route (TTF), TomTom shortest route (TTS), and TomTom eco routing (EcoTT).¹ See Supplementary Note 2 for details. Figure 1a-b shows how different navigation services may provide different either overlapping (a) or diverging (b) routes. This variation arises because the services rely on different criteria and possess diverse historical data on traffic conditions. We observe that the average overlap between the routes provided by these services ranges from 70% to 97% (see Supplementary Note 2). Note that these algorithms are black boxes to us since the implementation specifics of these services are unknown. We refer to a trip that follows a route suggested by a navigation service $s \in S$ as an s -routed trip.

To assess how a navigation service $s \in S$ affects traffic in a given city, we design controlled experiments [3] varying the rate of adoption of s in the range $r = 0\%, 10\%, 20\%, \dots, 100\%$. Given r , we assign $r\%$ of vehicles to a treatment group and the remaining $(100 - r)\%$ of vehicles to a control group. Vehicles in the treatment group are s -routed, while those in the control group follow a modified version of the fastest route on the road network computed by SUMO². This modification slightly lengthens the fastest route to account for the imperfections and irrational behaviour of human drivers [39] (see Methods and Supplementary Note 3). We assume that vehicles in the control group select their routes independently of one another, without knowing the choices of the other vehicles. For statistical robustness, the simulation for a given adoption rate r is repeated ten times, using different random compositions of the treatment and control groups in each run. Furthermore, we repeat all the above steps considering both low and high traffic loads. Low traffic loads refer to situations with few circulating vehicles in the city, such as off-peak hours and nighttime. High traffic load indicates that the traffic is approaching congestion, for example during peak hours. See Supplementary Note 4 for details.

We evaluate the impact of navigation services in isolation, where all the vehicles in the simulation use the same service, and in combination, where vehicles may choose among different services. We present only the isolation scenario because the results are analogous (Supplementary Note 5 shows results for the other scenarios). To assess the urban impact of navigation services, we evaluate route diversity, i.e., the number of road edges traversed at least once by any vehicle and the total CO2 emissions produced by the vehicles. We compute the CO2 emissions through a microscopic emission model provided by SUMO [34] that estimates the vehicle’s instantaneous emissions as a function of speed and acceleration (see Supplementary Note 6).

Our experimental setup has a main limitation that stems from interaction effects between vehicles on the road network [40]. The control group cannot be completely separated from the indirect effects of recommendations, as vehicles in the control group may encounter on the streets vehicles in the treatment group. Despite being a randomized controlled simulation, our experiments do not satisfy the Stable Unit Treatment Value Assumption from causal inference [41]. As a result, we cannot provide unbiased estimates of causal quantities of interest, such as the average treatment effect. This is a common scenario when conducting controlled experiments in complex social systems, which also applies to social media platforms [7]. Intuitively, we anticipate peer effects to reduce observable differences between the control and treatment groups. Therefore, our reported statistics likely underestimate the true causal effects of recommendations by navigation services.

¹AppleMaps, Waze, and Google Maps eco-routing are unavailable due to the absence of public APIs.

²<https://sumo.dlr.de/docs/duarouter.html>

Impact of navigation services

We conduct experiments in three cities in Italy: Florence, Milan, and Rome. These cities were chosen due to the availability of GPS traces to compute the mobility demand and their heterogeneity in size, population, and road network structure. For instance, Rome features an expansive road network with relatively long street segments and moderately winding roads. Milan is slightly smaller than Rome and is characterised by shorter street segments and a more regular network structure. Florence, the smallest, has the most winding and spatially intricate network. See Supplementary Table S1 for detailed statistics on the road networks.

Figure 2a-c illustrates the impact of varying the service adoption rate r on route diversity in the selected cities, considering high traffic loads. Results for low traffic loads are similar (see Supplementary Figure S1). If the navigation service had a negligible impact, we would expect a stable route diversity as r increases (horizontal dashed line in Figure 2a-c). Contrary to the assumption of insignificance, route diversity varies considerably with r following an exponential function (see Supplementary Note 7). When r is below a specific city- and service-dependent threshold ($\approx 25\text{-}50\%$), route diversity slightly increases by 0.15-1.05% in Florence, 0.08-0.34% in Milan, and 0.01-0.41% in Rome (see inset plots in Figure 2a-c) compared to the no-impact scenario ($r = 0\%$). On the other hand, when r exceeds this threshold, route diversity considerably decreases. At the total adoption rate ($r = 100\%$), route diversity is considerably reduced by 11.80-14.34% in Florence, 3.79-6.87% in Milan, and 9.73-14.26% in Rome compared to the no-impact scenario. We also examine the distribution of route diversity separately for vehicles in the treatment and control groups at various adoption rates. We find that vehicles in the treatment group exhibit significantly lower route diversity compared to vehicles in the control group, regardless of the adoption rate (see Supplementary Note 8).

These results demonstrate that increased adoption of navigation services reduces route diversity, leading to inefficient use of the road network. These trends are consistent under low and high traffic loads, with only minor fluctuations among navigation services. The reduction in route diversity emerges because navigation services tend to offer the same route to all vehicles with identical trips, leading to a concentration of traffic on fewer roads. This behaviour is exacerbated by the structure of the OD matrix, in which a small number of flows involve a large number of trips, while the majority involve fewer trips [42].

Figure 2d-f shows the average CO₂ emissions per vehicle produced at different adoption rates and traffic loads. When the traffic load is low, navigation services are generally beneficial: in most cases, CO₂ emissions are lower than they would be in the no-impact scenario (see Figure 2d-f), showing a near-linear decreasing trend with r . At the total adoption rate, navigation services can reduce CO₂ emissions by 2.15-5% in Florence and 6.64-11.13% in Milan. In Rome, some navigation services reduce CO₂ emissions by 0.26-3.69%, while GM, TTF and Bi slightly increase them by 2.4%, 1.13% and 1.57%, respectively.

However, at high traffic loads, the impact of navigation services depends on the adoption rate r . When r is low, CO₂ emissions decrease considerably; when r exceeds a certain city- and service-dependent threshold, the benefits plateau and in some cases CO₂ emissions increase (see Figure 2d-f). Note that as the adoption rate reaches $r = 100\%$ the overall CO₂ emissions become concentrated on a small fraction of roads due to the decreased route diversity, thereby increasing the inequality of distribution of CO₂ emissions on roads (see Supplementary Note 9). Figure 3a-c illustrates this effect in Milan for navigation service TTF: at a 0% adoption rate (Figure 3a), the traffic distribution is more even, whereas at a 100% adoption rate (3b), there is a concentration of traffic and CO₂ emissions on fewer roads. This effect is further illustrated by the increase in the Gini coefficient of CO₂ emissions across roads at $r = 0\%$, $r = 50\%$, and $r = 100\%$ adoption rates (see Figure 3d-f and Supplementary Figure S11). In Florence and Milan, emissions are more evenly distributed at 50% adoption than at 0% or 100%, reflecting a temporary rise in route diversity before route convergence takes hold. At 100% adoption, emissions become significantly more concentrated: the Gini coefficient increases by 0.023 in Florence, 0.025 in Milan, and 0.031 in Rome compared to 50% adoption. This corresponds to an additional 2.04% (Florence), 2.31% (Milan), and 3.9% (Rome) of total CO₂ emissions being concentrated on the top 20% most polluted roads.

Across all cities, we observe a consistent shift of routes, and consequently CO₂ emissions, toward high-capacity infrastructures such as highways and major arterial corridors (attractors). These attractors are designed to accommodate large traffic volumes and are often favoured by navigation algorithms aiming to minimise travel time. Although attractors account for only about 6% of the total road network in each city, they absorb a disproportionately large share of CO₂ emissions, and this imbalance intensifies with higher adoption rates (see Figure 3g-i). From 0% to 100% adoption, the share of emissions on attractor roads rises from 17.61% to 36.25% in Florence, 9.94% to 26.42% in Milan, and 26.02% to 33.66% in Rome. Therefore, navigation services exacerbate the burden on already “grossly polluted roads” [43], making them even more heavily trafficked and environmentally degraded. The full breakdown of CO₂ emissions by road type is provided in Supplementary Note 10.

In Florence, the most effective adoption rate for all navigation services is around $r = 70\text{-}80\%$, resulting in an average CO₂ reduction of about 27%; after this point, the benefits diminish (see Figure 2d). In Milan, GM and TomTom-based services (TTF, TTS, and ecoTT) consistently reduce CO₂ emissions as r increase, achieving reductions of approximately 19-22% at the total adoption rate. In contrast, MB and Bi reach their highest reductions ($\approx 12\%$) when $r = 60\%$ and $r = 70\%$, respectively; beyond these rates, the benefits considerably diminish (CO₂ reductions decrease by 9%). In Rome, optimal adoption rates vary by service: 20% for Bi, 40% for MB, GM and TTF, 60% for TTS, and 70% for ecoTT, leading to an average CO₂ reduction of 3.29%. Notably, Bi, MB, GM and TTF in Rome lead to increased CO₂ emissions beyond certain thresholds compared to the baseline scenario: 9.10% for Bi, 4.61% for MB, 2.22% for GM and 0.52% for TTF (see Supplementary Table S2 for details on the CO₂ reductions).

Our results reveal that even an eco-routing service (EcoTT) shows CO₂ trends similar to the other navigation services (see brown squares in Figure 2). This suggests that relying solely on eco-routing is inadequate for fully controlling the impact of algorithmic urban recommendations. Being eco-friendly is not just a property of an individual route but also of drivers’ aggregate behaviour.

We also explore the relationship between route diversity and total CO₂ emissions during periods of high traffic load by examining the correlation between ΔD_r and ΔE_r . Here, ΔD_r represents the marginal change in route diversity, while ΔE_r denotes the marginal change in CO₂ emissions. We compute ΔD_r as the difference in route diversity values between adoption rates $r - 10\%$ and r . Similarly, ΔE_r is the difference in CO₂ emissions over the same interval. A positive ΔE_r indicates a decrease of CO₂ emissions at adoption rate r compared to $r - 10\%$, whereas a positive ΔD_r indicates a decrease of route diversity at r compared to $r - 10\%$.

In Florence, Spearman’s rank correlation coefficient is $\rho = -0.958$; in Milan, it is $\rho = -0.882$, and in Rome, it is $\rho = -0.899$. This relationship is well described by an exponential decay function: $\Delta E_r = \alpha e^{-\beta \Delta D_r} + \gamma$. In this formula, the coefficient β measures how quickly incremental CO₂ changes (ΔE_r) respond to incremental changes in route diversity (ΔD_r). A higher β indicates a more rapid CO₂ change per unit change in route diversity. Milan has the highest coefficient value ($\beta = 0.0068$), indicating that changes in route diversity have a more significant impact on CO₂ reduction compared to Florence ($\beta = 0.00313$) and Rome ($\beta = 0.00226$).

Figure 4a-c illustrates this trend. At low adoption rates, slight increases in route diversity (i.e., a negative ΔD_r , highlighted in grey) lead to substantial reductions in CO₂ emissions. As r increases, small reductions in route diversity result in moderate CO₂ reductions. However, as ΔD_r further increases, ΔE_r decreases, indicating a diminishing return effect. This pattern is consistent across all cities and navigation services (Figure 4d-f), suggesting that while initial efforts to optimize routes are highly effective, their efficiency decreases as further reductions in route diversity yield progressively smaller CO₂ reduction benefits. Therefore, the positive impact of navigation services on reducing CO₂ emissions diminishes as route diversity decreases.

Core driving factors of concentration patterns

Navigation services reduce route diversity, amplifying the concentration of traffic and CO₂ emissions on fewer roads. To better understand the phenomenon, we investigate whether its key effects emerge independently of the structural complexity of real-world cities. We do that by replicating our experiments on a simplified road network and two flow configurations. This abstraction allows us to isolate the core dynamics of the phenomenon. In this scenario, routed vehicles follow the fastest route – as a proxy for navigation service recommendations – while non-routed vehicles follow slightly perturbed variations of this optimal route. All roads are bidirectional and have identical speed limits, ensuring uniform travel conditions across the entire road network.

We first simulate a single OD flow on a 10×10 grid network (see Figure 5a), where all vehicles share the same origin and destination and vary the adoption rate as in the experiments on real cities. We find that, as the adoption rate increases, route diversity declines but CO₂ emissions continue to decrease steadily (see Supplementary Figure S24). This suggests that reduced route diversity alone does not necessarily lead to inefficiencies, likely due to the limited interactions among vehicles in this simplified setting.

To enforce vehicle interactions, we simulate two orthogonal OD flows on the same grid (see Figure 5b). The fastest routes of these flows intersect at the centre of the grid, causing vehicles to converge at shared crossroads and triggering congestion. Despite its simplicity, this setup reproduces all key patterns observed in real cities as the adoption rate approaches full adherence (see Figure 5c-e): a sharp reduction in route diversity (c), a plateau in CO₂ emissions (d), and a nonlinear relationship between ΔD_r and ΔE_r (e). The simplified setting also captures the rise in CO₂ inequality as adoption approaches 100%, with the increasing Gini coefficient aligning closely with the patterns observed in real cities (see Supplementary Figure S30). We extend the analysis to a larger grid and randomised grid-like networks to verify that our results are not an artefact of the road network size and regularity. We find that the same patterns persist (see Supplementary Figures S25–S31). Full experimental details, including grid configurations, randomised network generation, and additional scenarios, are provided in Supplementary Note 11.

The emergence of traffic and emissions concentration, even in a minimal setting, suggests that the patterns observed are not tied to specific urban features and are likely to generalise across a broad range of city contexts.

Discussion

Navigation services may offer benefits under certain conditions, but they also reshape traffic patterns, environmental quality, and social equity within urban ecosystems. In all the real-world cities we analysed, as well as in our simplified city scenarios, a consistent pattern emerged: as adoption rates increase, traffic and CO₂ emissions become increasingly concentrated on a smaller subset of roads – a consequence of reduced route diversity. These roads are typically highways and major arterial corridors, where CO₂ concentrations are further intensified. This spatial concentration carries significant implications for urban policy, the governance of digital platforms, and human-AI interaction.

The first major consequence is the amplification of urban inequality. As navigation services redistribute traffic, some neighbourhoods are burdened with disproportionate levels of congestion and pollution, while others remain largely unaffected. Roads absorbing higher volumes of vehicles may experience declines in property values and quality of life, while areas bypassed by traffic may lose footfall and customer revenue. Moreover, navigation services may conflict with municipal routing strategies designed to protect sensitive areas – such as schools, hospitals, and parks – thereby undermining carefully crafted safety and equity policies. The severe congestion experienced in Leonia and Italian mountain villages highlights how algorithmic routing can rapidly disrupt local traffic patterns.

Second, the relevance of our study extends beyond navigation services alone. Recent research on car-sharing and ride-hailing platforms has linked these services to increased congestion and emissions, reduced public transport usage, and growing concerns around social equity [3, 44, 16]. However, much like the literature on navigation services, these

studies tend to focus on specific platforms and individual urban contexts. Our simulation framework, being both data-driven and city-agnostic, can be readily adapted to assess the impact of these mobility services as a function of their adoption rate, and to evaluate potential strategies for mitigating their unintended consequences.

Finally, this work contributes to the broader discussion on human–AI coevolution [1]. Navigation services operate within a dynamic feedback loop: traffic patterns influence algorithmic recommendations; these recommendations shape drivers’ route choices, and those choices, in turn, alter future traffic patterns. Our study reveals a strong interdependence between adoption rate, route diversity, and CO₂ emissions within this loop. The next step is to understand how this relationship evolves over time as both individuals and navigation services continuously adapt to one another. Such insights will be crucial for designing online platforms that are not only efficient, but also equitable and sustainable in the long run.

Our study can be easily reproduced in any city, as it only requires widely available data on the city’s mobility demand and road network, as well as publicly accessible navigation services’ APIs. Upcoming legislation, such as the EU’s Digital Services Act and Digital Market Act [33], mandates the introduction of transparency measures on the algorithms used by very large online platforms, including navigation services, for recommending content or products to users. In this regard, our study marks an initial stride towards systematically assessing algorithmic influence on urban ecosystems and a conceptual and methodological foundation for agile responses to collective goal challenges. By understanding and managing the relationship between drivers and navigation services, we have the potential to anticipate the level of emissions in our urban environments and take immediate, informed actions when they overcome a certain tolerance threshold. This is crucial because the decisions made by policymakers rely on the accuracy of our measurements and the promptness of our response to these measurements.

Methods

Road Networks. We model a city’s road network as a directed weighted multigraph $G = (V, E)$, where V denotes the set of nodes representing intersections, and E is a multiset of edges representing the road segments connecting the vertices. Each edge $e_{i,j} \in E$, with $i, j \in V$, is associated with its minimum expected travel time $t(e_{i,j})$, capacity $c(e_{i,j})$, and speed limit $s(e_{i,j})$.

We extract the road networks using OSM Web Wizard, which retrieves and pre-processes road network data from OpenStreetMap (OSM). Following the approach described in [45], we manually fine-tune the road networks to correct inaccuracies that could potentially cause deadlocks and other unrealistic behaviours, thus negatively impacting the simulations. This fine-tuning phase includes correcting lane number inaccuracies, addressing road continuity disruptions, and modifying turns to align with real-world conditions. We use Google Maps and StreetView as benchmarks to ensure the accuracy of these adjustments.

Traffic simulator. SUMO (Simulation of Urban MObility) is an open-source agent-based traffic simulator allowing intermodal traffic simulation, including road vehicles, public transport, and pedestrians [34]. It simulates each vehicle’s dynamics, considering interactions with other vehicles, traffic jams, queues at traffic lights, and slowdowns caused by heavy traffic, supporting various route choice methods and routing strategies [45].

To simulate a traffic scenario, SUMO requires two input elements: a road network and a traffic demand. The road network describes the virtual road infrastructure where simulated vehicles move during the simulation. The traffic demand outlines the vehicles’ movement on the road network. We describe a vehicle’s movements as a route, i.e., a sequence of interconnected edges linking an origin to a destination and a departure time.

SUMO can simulate vehicular pollutant emissions utilizing the HBEFA3 emission model derived from the Handbook of Emission Factors for Road Transport (HBEFA) database [46]. The HBEFA3-based model estimates the vehicle’s instantaneous CO₂ emissions relying on the following function, which is linked to the power the vehicle’s engine

produces in each trajectory point j to overcome the driving resistance force [46]:

$$\mathcal{E}(j) = c_0 + c_1sa + c_2sa^2 + c_3s + c_4s^2 + c_5s^3$$

where s and a are the vehicle’s speed and acceleration in point j , respectively, and c_0, \dots, c_5 are parameters specific to each emission type and vehicle taken from the HBEFA database. In this work, we use SUMO version 1.19.0.

Navigation services APIs. Vehicles in the treatment group follow routes suggested by various navigation services. We utilise a collection of widely-used navigation services with publicly accessible APIs, including Bing Maps (Bi), MapBox (MB), TomTom eco routing (EcoTT), TomTom fastest route (TTF), and TomTom short (TTS). These services provide routes between an origin and a destination at a specified departure time, considering various factors, such as typical traffic conditions at the time of departure. The rationale behind selecting these specific navigation services is based on their popularity, availability of public APIs, and variety in routing criteria, which provide a broad perspective on route suggestions. Additionally, these services cover many routing preferences, from eco-friendly to the fastest and shortest routes, offering a comprehensive comparison. Table 1 presents a detailed overview of the key characteristics of each navigation service, including the service name, service provider, whether it accounts for historical traffic, the name of the profile used (i.e., the routing criteria), a description, and the URL of the reference documentation.

As the route recommendations from the APIs are typically provided as sequences of GPS points, we employ a map-matching procedure to integrate these routes into the SUMO simulator. Specifically, we apply the state-of-the-art Longest Common Subsequence (LCSS) algorithm [47] to convert the sequence of GPS points into a sequence of connected edges in the SUMO road network, accurately representing the suggested routes.

Modified fastest route. Vehicles in the control group follow a modified version of the fastest route implemented by SUMO’s duarouter algorithm.³ Duarouter is a tool for simulating human driving and routing behaviour. It computes vehicle routes with an adjustable degree of variability, controlled by a parameter $w \in [1, +\infty)$. When $w = 1$, duarouter calculates the standard fastest route on the road network. When $w > 1$, it dynamically alters the edge weights (expected travel time) by a random factor uniformly drawn from the interval $[1, w)$. This random process ensures that different vehicles may get different routes even if their trip has the same origin and destination. As w increases, the extent of randomness in the route calculation also increases, resulting in routes that can diverge significantly from the fastest route (see Supplementary Note 3). This increased route variability helps us model the imperfections of human driving behaviour, which often deviates from the fastest route due to personal preferences, lack of complete knowledge of the road network, and irrational behaviours [39, 48]. In our experiments, we set $w = 5$ to introduce a moderate level of randomness in the control group’s routing. To assess the robustness of this choice, we also perform simulations using $w = 3$ and $w = 7$, corresponding to lower and higher levels of variability. As detailed in Supplementary Note 3, the results remain qualitatively and quantitatively consistent across these settings, demonstrating that our findings are not sensitive to the specific choice of w .

GPS Data. To estimate each city’s mobility demand, we use a vehicular GPS trajectory dataset provided by OCTO, a company that provides a data collection service for insurance companies. This dataset describes the trajectories of thousands of vehicles for various Italian localities over an entire year. While the market penetration of the dataset varies, it generally represents a minimum of 2% of the total registered vehicles. Our analysis focuses on the cities of Florence, Milan, and Rome, selected due to the availability of GPS traces suitable for computing origin-destination (OD) matrices, their diverse sizes, populations, and road network structures. The raw dataset includes 7,102,351 GPS points from 24,640 vehicles in Florence, 143,698,720 GPS points from 106,456 vehicles in Milan, and 26,801,872 GPS points from 30,763 vehicles in Rome. The dataset’s validity and reliability are corroborated by its extensive use in prior studies [49, 50, 43].

³<https://sumo.dlr.de/docs/duarouter.html>

We process the raw GPS dataset to create segmented trajectories that represent semantic journeys as follows:

- We eliminate noise by filtering out GPS points with speeds exceeding 250 km/h [51];
- We use a stop detection algorithm [51, 37] to segment each trajectory into sub-trajectories based on identified stops. A stop is identified when a vehicle remains within a distance of 0.2 km from a trajectory point for at least 20 minutes;
- We consider only trips that start and end within the predefined area of interest. For trips that start or end outside this area but traverse it, we used the first entry point within the area as the origin and the last exit point as the destination. This method preserves commuter trips originating or ending outside the city.

To compute the OD matrix reflecting a city’s traffic patterns, we first discretize the city into 1 km² squared tiles using scikit-mobility [37]. We then extract flows from the pre-processed segmented trajectories to fit the OD matrix.

We compute the flows by considering only trips with a duration between 5 and 60 minutes that depart during the morning peak hours on all Wednesdays. Focusing on morning peak hours allows us to model high-traffic scenarios, as they represent periods of intense traffic congestion. By selecting Wednesdays, we ensure the capture of typical weekday traffic, avoiding anomalies associated with weekends or specific weekdays with unique traffic patterns. We exclude outlier weeks (e.g., holidays) from the analysis. Additionally, we filter out infrequent flows, retaining only those that occur regularly. See Supplementary Note 1 for further details on the pre-processing and flow computation.

After the pre-processing step, the dataset used to compute the OD matrix includes 5,477 trips from 1,184 vehicles for Florence (616 distinct flows); 113,323 trips from 15,997 vehicles for Milan (11,967 distinct flows); and 13,647 trips from 1,965 vehicles for Rome (1,757 distinct flows).

For each city, based on the pre-processed data, we obtain an origin-destination matrix M , where an element $m_{o,d} \in M$ denotes the number of trips that start in tile o and end in tile d . Each vehicle’s trip starting and ending tiles determine the origins and destinations.

	provider	profile name	profile description	url
Bi	Bing Maps	timeWithTraffic	optimization of travel time using current traffic information.	bit.ly/ref_b
MB	Mapbox	driving-traffic	lowest probability of slowdowns given current and historical traffic conditions.	bit.ly/ref_mb
ecoTT	TomTom	eco	trade-off between travel time and fuel consumption	bit.ly/ref_tt
TTF	TomTom	fastest	shortest travel time while keeping the routes sensible.	bit.ly/ref_tt
TTS	TomTom	short	trade-off between travel time and travel distance.	bit.ly/ref_tt
GM	Google Maps	not available	not available	bit.ly/ref_gm

Table 1: Characteristics of navigation services' APIs: service provider, routing criteria (profile name), description of the routing strategy, and URL with the documentation.

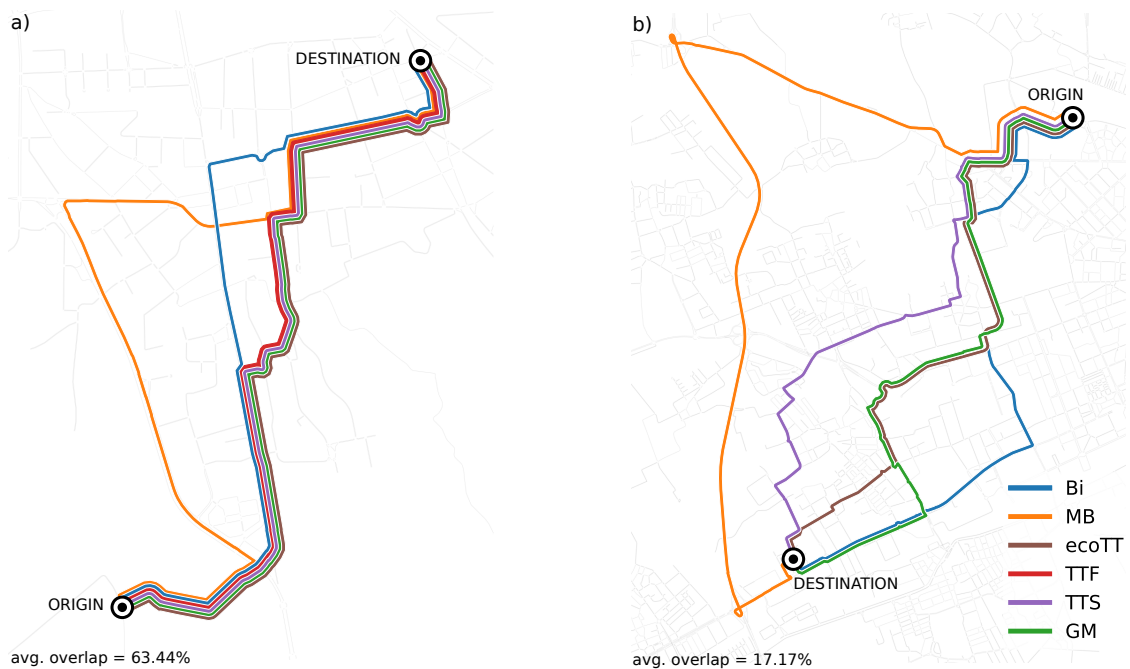


Figure 1: **Routes recommended by navigation services.** (a, b) Two origin-destination pairs in Milan and the corresponding routes suggested by different navigation services. Panel (a) shows a case where recommendations largely overlap (average overlap = 63.44%), while panel (b) illustrates a case with significant divergence (average overlap = 17.17%). This variation occurs because the services rely on different criteria and possess diverse historical data on traffic conditions.

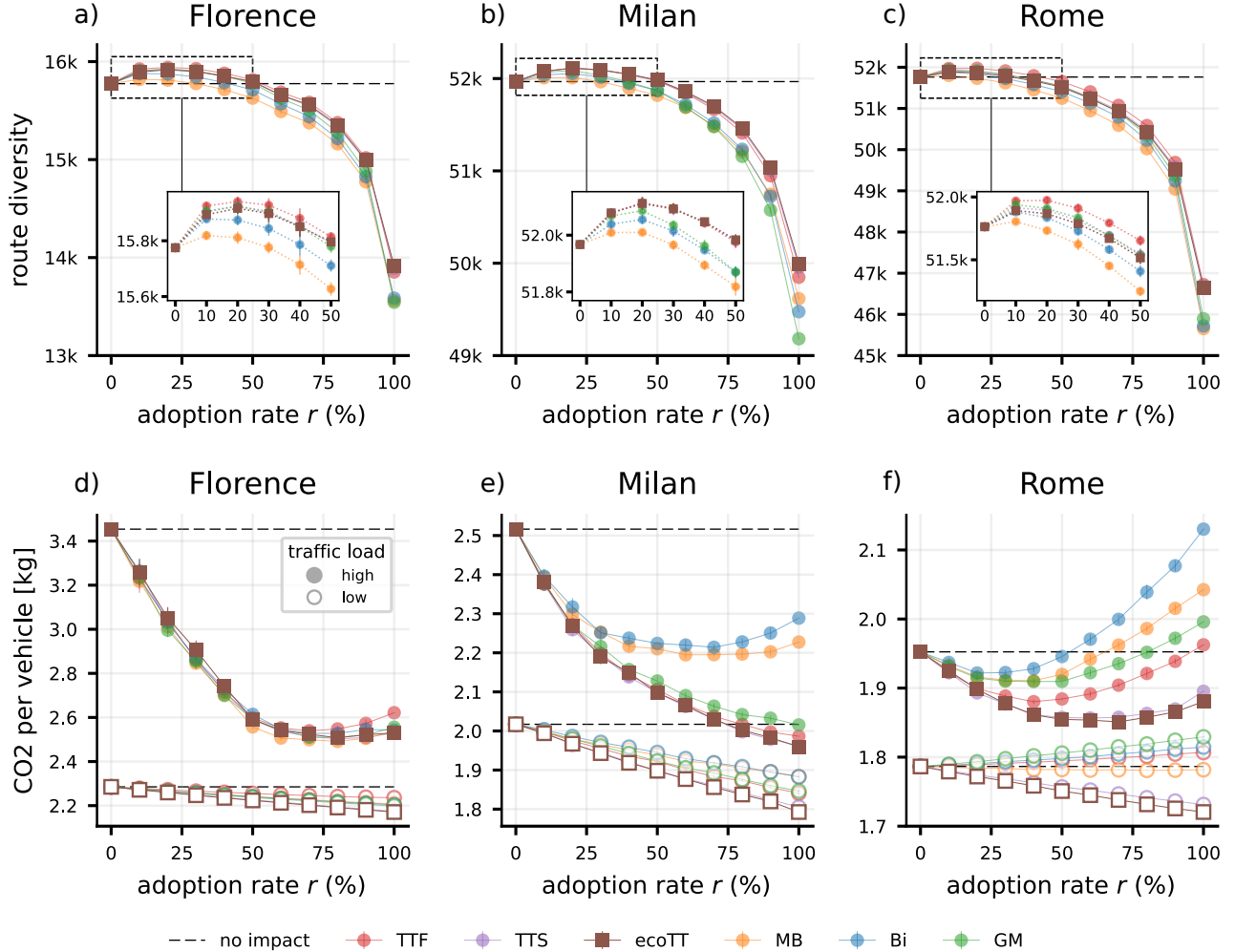


Figure 2: **Impact of navigation services on route diversity and CO2 emissions.** (a-c) Service adoption rate (r) versus route diversity at high traffic loads in Florence, Milan, and Rome. The dashed line represents the no-impact scenario ($r=0\%$). Markers indicate the average route diversity over ten simulations with different random choices of s -routed vehicles. Squares refer to the navigation service ecoTT, which employs eco-routing. Vertical bars indicate the standard deviation. The inset plots zoom on the range $r = 0\%, \dots, 50\%$, where route diversity slightly increases. Increased adoption of navigation services reduces route diversity, with only minor fluctuations among navigation services. (d-f) Service adoption rate (r) versus average CO2 emissions per vehicle at high (filled markers) and low (empty markers) traffic loads. The dashed line represents the no-impact scenario ($r = 0\%$). Markers indicate the average CO2 emissions over ten simulations with different random choices of s -routed vehicles. Squares refer to ecoTT. Vertical bars indicate the standard deviation. At high traffic loads, when r is low, CO2 emissions decrease considerably; when r exceeds a certain city- and service-dependent threshold, the benefits plateau and, in some cases, even reverse.

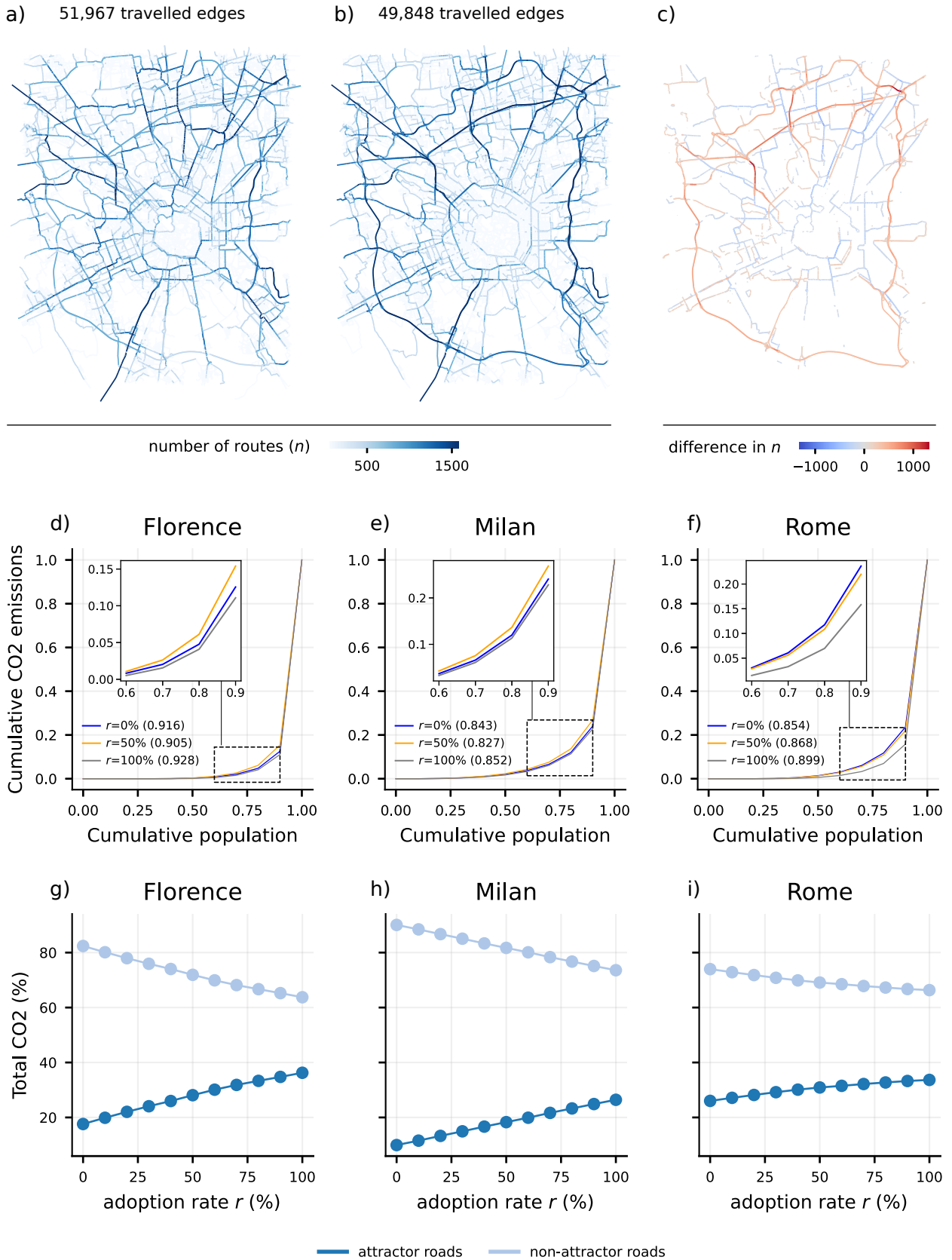


Figure 3

Figure 3. Road usage of navigation services. (a, b) Route distribution of trips in Milan with TomTom Fastest (TTF) at adoption rates $r=0\%$ (a) and $r = 100\%$ (b). Darker edges indicate higher traffic concentration. Traffic is concentrated on fewer road edges at $r=100\%$. (c) Difference in road usage between $r = 100\%$ and $r = 0\%$. Blue edges indicate segments where traffic decreases under full adoption of TTF; red edges highlight segments where traffic increases. (d–f) Gini coefficient of CO2 emissions across roads at $r = 0\%$, 50%, and 100%. Emissions are most equally distributed at 50% adoption but become increasingly concentrated at full adoption. (g–i) Share of total CO2 emissions produced on major attractor roads (e.g., highways and arterial corridors) as adoption increases. Despite representing only $\approx 6\%$ of the road network, these roads absorb a disproportionate and growing share of emissions.

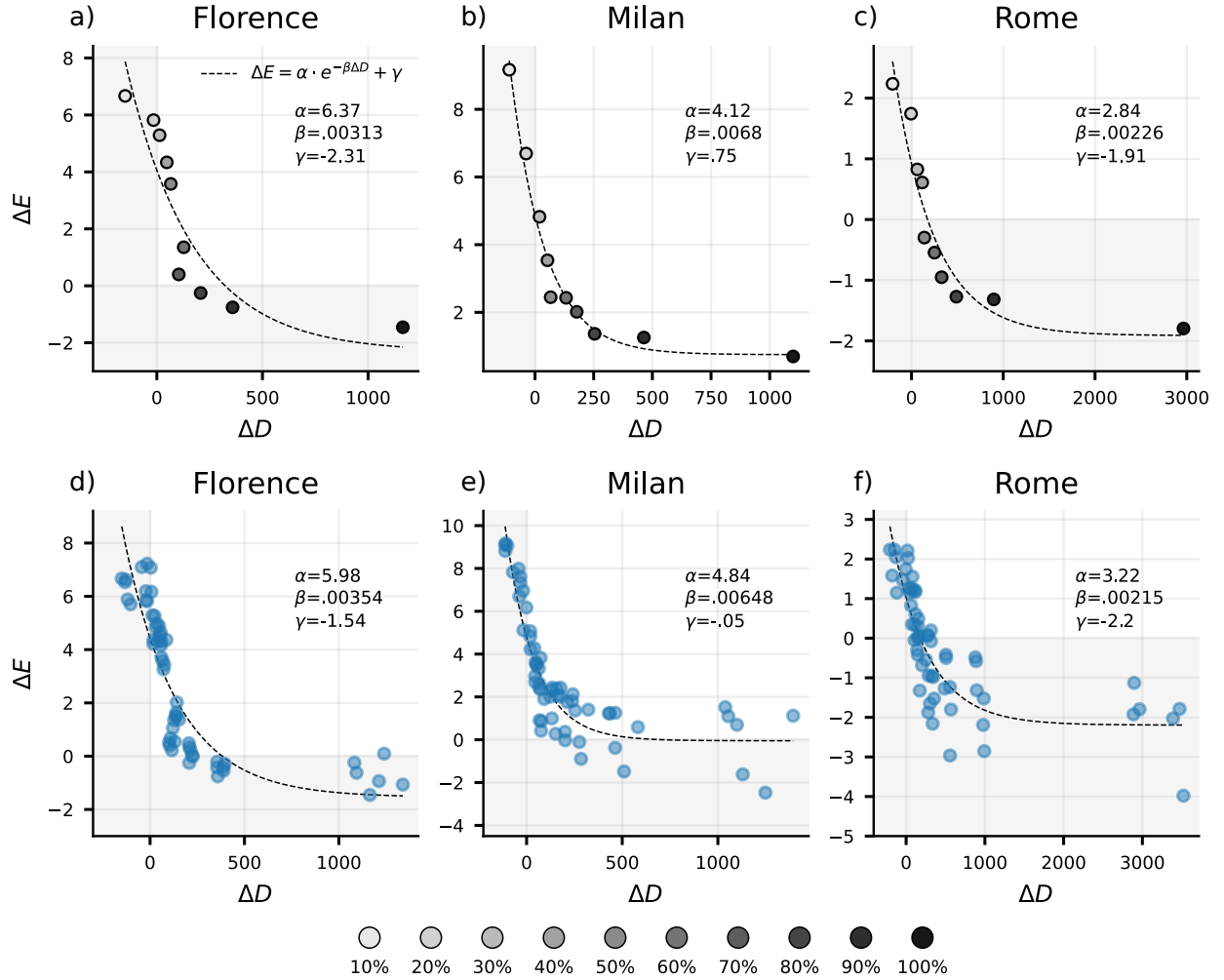


Figure 4: **Relationship between route diversity and CO2 emissions.** (a-c) The relationship between the marginal change in route diversity (ΔD) and the marginal change in CO2 emissions (ΔE) for TTF in Florence, Milan, and Rome. We find similar results for the other navigation services. The points are shaded from light grey to black, representing the service adoption rate (from $r=10\%$ to $r=100\%$). (d-f) Same relationship for all navigation services. Regions where ΔD or ΔE are negative are highlighted in grey. The black dashed line represents the exponential decay fit for each scenario. At low adoption rates, slight increases in route diversity lead to substantial reductions in CO2 emissions. As r increases, small reductions in route diversity result in moderate CO2 reductions. However, as ΔD further increases, ΔE decreases, indicating a diminishing return effect. This pattern is consistent across all cities and navigation services.

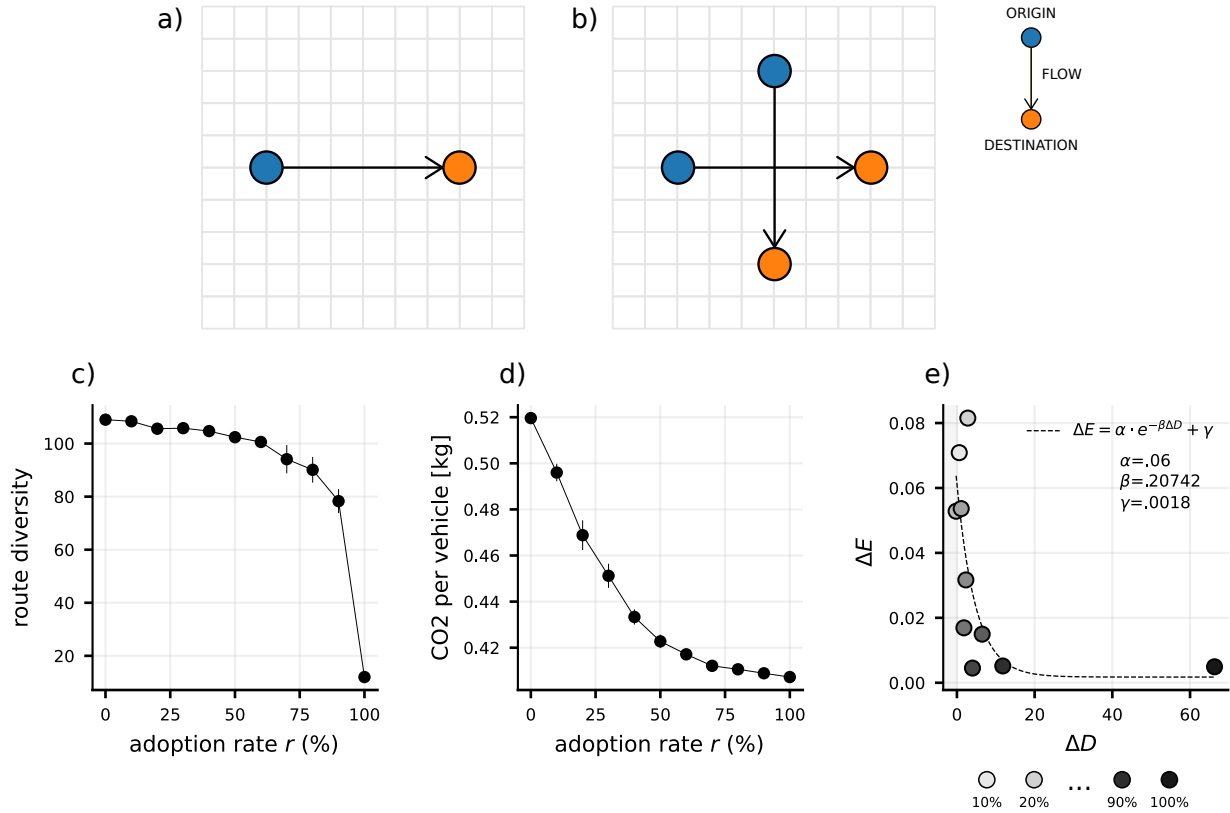


Figure 5: **Impact of navigation service adoption in a simplified setting.** (a, b) Schematic of a 10x10 grid network with synthetic OD flows. Panel (a) shows a single OD flow; panel (b) introduces two intersecting OD flows that increase vehicle interactions at the grid centre. Routed vehicles follow the fastest route, while non-routed vehicles take perturbed variants. (c) Route diversity as a function of adoption rate r . With two OD flows, route diversity decreases rapidly as r increases, replicating patterns observed in real cities. (d) Average CO2 emissions per vehicle versus adoption rate. Emissions initially decline, then plateau due to increased congestion at shared intersections. (e) Marginal relationship between changes in route diversity (ΔD) and CO2 emissions (ΔE), showing a nonlinear trend consistent with urban scenarios. Points are shaded from light grey to black to represent increasing adoption rates from $r = 10\%$ to $r = 100\%$.

Data availability statement The processed road networks for Florence, Milan, and Rome utilized in this study are accessible at <https://github.com/GiulianoCornacchia/Urban-Impact-Navigators>. The OCTO dataset used in our research is proprietary and thus not publicly available. Consequently, we cannot provide the original OD matrices derived from this dataset. To overcome this limitation, we have provided the necessary code to generate an OD matrix for Milan utilizing a publicly accessible dataset available at https://ckan-sobigdata.d4science.org/dataset/gps_track_milan_italy. Additionally, we provide a routine to create random OD matrices, which can be helpful in scenarios where trajectory data is unavailable.

Due to proprietary restrictions, the specific navigation service suggestions used in our study cannot be included. However, we have included code to generate the fastest route, replicating the functionality of a navigation service prototype. This code also includes routines to generate perturbations of the fastest routes for non-routed vehicles.

Code availability statement The Python code for replicating the analyses in the study is publicly available at <https://github.com/GiulianoCornacchia/Urban-Impact-Navigators>.

Acknowledgements GC and LP have been partially supported by PNRR (Piano Nazionale di Ripresa e Resilienza) in the context of the research program 20224CZ5X4 PE6 PRIN 2022 “URBAI – Urban Artificial Intelligence” (CUP B53D23012770006), funded by the European Commission under the Next Generation EU programme. MN and DP have been partially supported by PNRR - M4C2 - Investimento 1.3, Partenariato Esteso PE00000013 - “FAIR – Future Artificial Intelligence Research” – Spoke 1 “Human-centered AI”, funded by the European Commission under the NextGeneration EU programme. We thank Daniele Fadda for his precious support with data visualisation.

Author contributions GC conceptualised the work, developed the simulation framework, performed the experiments, designed and made the plot and wrote the paper. LP conceptualised the work, designed the experiments, designed the plots, wrote the paper, and supervised the research. MN conceptualised the work. DP conceptualised the work and wrote the paper. All authors read and approved the paper.

Competing interests The authors declare no competing interests.

Corresponding authors The corresponding authors are G.C. (giuliano.cornacchia@phd.unipi.it) and L.P. (luca.pappalardo@isti.cnr.it)

References

- [1] Pedreschi, D. *et al.* Human-ai coevolution. *Artificial Intelligence* 104244 (2024).
- [2] Tsvetkova, M., Yasseri, T., Pescetelli, N. & Werner, T. A new sociology of humans and machines. *Nature Human Behaviour* **8**, 1864–1876 (2024).
- [3] Pappalardo, L. *et al.* A survey on the impact of ai-based recommenders on human behaviours: methodologies, outcomes and future directions. *arXiv preprint arXiv:2407.01630* (2024).
- [4] Pappalardo, L., Manley, E., Sekara, V. & Alessandretti, L. Future directions in human mobility science. *Nature Computational Science* (2023). URL <https://doi.org/10.1038/s43588-023-00469-4>.
- [5] Wagner, C. *et al.* Measuring algorithmically infused societies. *Nature* **595**, 197–204 (2021).
- [6] Sîrbu, A., Pedreschi, D., Giannotti, F. & Kertész, J. Algorithmic bias amplifies opinion fragmentation and polarization: A bounded confidence model. *PLOS ONE* **14**, e0213246 (2019).
- [7] Huszár, F. *et al.* Algorithmic amplification of politics on twitter. *Proceedings of the National Academy of Sciences* **119** (2022).

- [8] Perra, N. & Rocha, L. E. C. Modelling opinion dynamics in the age of algorithmic personalisation. *Scientific Reports* **9**, 7261 (2019).
- [9] Bakshy, E., Messing, S. & Adamic, L. A. Exposure to ideologically diverse news and opinion on facebook. *Science* **348**, 1130–1132 (2015).
- [10] Waller, I. & Anderson, A. Quantifying social organization and political polarization in online platforms. *Nature* **600**, 264–268 (2021).
- [11] Cinelli, M., De Francisci Morales, G., Galeazzi, A., Quattrociocchi, W. & Starnini, M. The echo chamber effect on social media. *Proceedings of the National Academy of Sciences* **118**, e2023301118 (2021).
- [12] Chen, W., Pacheco, D., Yang, K.-C. & Menczer, F. Neutral bots probe political bias on social media. *Nature communications* **12**, 5580 (2021).
- [13] Kleinberg, J., Ludwig, J., Mullainathan, S. & Sunstein, C. R. Algorithms as discrimination detectors. *Proceedings of the National Academy of Sciences* **117**, 30096–30100 (2020).
- [14] Mehrabi, N., Morstatter, F., Saxena, N., Lerman, K. & Galstyan, A. A survey on bias and fairness in machine learning. *ACM Computing Surveys* **54**, 1–35 (2021).
- [15] Lee, D. & Hosanagar, K. How do recommender systems affect sales diversity? a cross-category investigation via randomized field experiment. *Information Systems Research* **30**, 239–259 (2019).
- [16] Yan, A. & Howe, B. Fairness-Aware demand prediction for new mobility. In *Proceedings of the AAAI Conference on Artificial Intelligence*, vol. 34, 1079–1087 (2020).
- [17] Brantingham, P. J. The logic of data bias and its impact on place-based predictive policing. *Ohio State Journal of Criminal Law* (2017).
- [18] Howe, B. *et al.* Integrative urban AI to expand coverage, access, and equity of urban data. *The European Physical Journal Special Topics* **231**, 1741–1752 (2022). URL <https://doi.org/10.1140/epjs/s11734-022-00475-z>.
- [19] Macfarlane, J. Your navigation app is making traffic unmanageable. *IEEE Spectrum* 22–27 (2019).
- [20] Siuhi, S. & Mwakalonge, J. Opportunities and challenges of smart mobile applications in transportation. *Journal of Traffic and Transportation Engineering* **3**, 582–592 (2016).
- [21] Foderaro, L. W. Navigation apps are turning quiet neighborhoods into traffic nightmares. *The New York Times* .
- [22] RaiNews. I sindaci dell’alto adige contro google maps: tutta colpa dei furbetti della coda (2024). Accessed: 2024-04-18.
- [23] Hendrix, S. Traffic-weary homeowners and waze are at war, again. guess who’s winning. *The Washington Post* (2016).
- [24] McCarty, M. The road less traveled? not since waze came to los angeles. *NPR All Tech Considered* (2016).
- [25] Cornacchia, G. *et al.* How routing strategies impact urban emissions. In *Proceedings of the 30th International Conference on Advances in Geographic Information Systems*, 1–4 (2022).
- [26] Arora, N. *et al.* Quantifying the sustainability impact of google maps: A case study of salt lake city (2021). 2111.03426.
- [27] Barth, M., Boriboonsomsin, K. & Vu, A. Environmentally-friendly navigation. In *2007 IEEE Intelligent Transportation Systems Conference*, 684–689 (2007).
- [28] Ahn, K. & Rakha, H. A. Network-wide impacts of eco-routing strategies: A large-scale case study. *Transportation Research Part D: Transport and Environment* **25**, 119–130 (2013). URL <https://www.sciencedirect.com/science/article/pii/S1361920913001259>.

- [29] Valdes, C., Perez-Prada, F. & Monzon, A. Eco-routing: More green drivers means more benefits. In *Proceedings of the XII Conference on Transport Engineering, Valencia, Spain, 7–9* (2016).
- [30] Perez-Prada, F., Monzón, A. & Valdés, C. Managing traffic flows for cleaner cities: The role of green navigation systems. *Energies* **10**, 791 (2017).
- [31] Thai, J., Laurent-Brouty, N. & Bayen, A. M. Negative externalities of gps-enabled routing applications: A game theoretical approach. In *2016 IEEE 19th International Conference on Intelligent Transportation Systems (ITSC)*, 595–601 (2016).
- [32] Johnson, I., Henderson, J., Perry, C., Schöning, J. & Hecht, B. Beautiful... but at what cost? an examination of externalities in geographic vehicle routing. *Proc. ACM Interact. Mob. Wearable Ubiquitous Technol.* **1** (2017). URL <https://doi.org/10.1145/3090080>.
- [33] Regulation (eu) 2022/2065 of the european parliament and of the council of 19 october 2022 on a single market for digital services and amending directive 2000/31/ec (digital services act). <https://eur-lex.europa.eu/legal-content/EN/TXT/?uri=CELEX:32022R2065> (2022). Accessed via EUR-Lex.
- [34] Lopez, P. A. *et al.* Microscopic traffic simulation using sumo. In *2018 21st International Conference on Intelligent Transportation Systems (ITSC)*, 2575–2582 (2018).
- [35] Hazelton, M. L. Inference for origin–destination matrices: estimation, prediction and reconstruction. *Transportation Research Part B: Methodological* **35**, 667–676 (2001).
- [36] Cerqueira, S., Arsenio, E. & Henriques, R. Inference of dynamic origin–destination matrices with trip and transfer status from individual smart card data. *European Transport Research Review* **14**, 1–18 (2022).
- [37] Pappalardo, L., Simini, F., Barlacchi, G. & Pellungrini, R. scikit-mobility: A Python Library for the Analysis, Generation, and Risk Assessment of Mobility Data. *Journal of Statistical Software* **103**, 1–38 (2022). URL <https://www.jstatsoft.org/index.php/jss/article/view/v103i04>.
- [38] Bonnel, P., Fekih, M. & Smoreda, Z. Origin-destination estimation using mobile network probe data. *Transportation Research Procedia* **32**, 69–81 (2018).
- [39] Seele, S., Dettmar, T., Herpers, R., Bauckhage, C. & Becker, P. Cognitive aspects of traffic simulations in virtual environments. *SNE Simul. Notes Eur.* **22** (2012).
- [40] Aronow, P. M. & Samii, C. Estimating average causal effects under general interference, with application to a social network experiment. *The Annals of Applied Statistics* **11**, 1912–1947 (2017). URL <http://www.jstor.org/stable/26362172>.
- [41] Cox, D. R. Planning of experiments. (1958).
- [42] Barbosa, H. *et al.* Human mobility: Models and applications. *Physics Reports* **734**, 1–74 (2018).
- [43] Böhm, M., Nanni, M. & Pappalardo, L. Gross polluters and vehicle emissions reduction. *Nature Sustainability* 1–9 (2022).
- [44] Ngo, N. S., Götschi, T. & Clark, B. Y. The effects of ride-hailing services on bus ridership in a medium-sized urban area using micro-level data: Evidence from the lane transit district. *Transport Policy* **105**, 44–53 (2021).
- [45] Argota Sánchez-Vaquerizo, J. Getting real: The challenge of building and validating a large-scale digital twin of barcelona’s traffic with empirical data. *ISPRS International Journal of Geo-Information* **11** (2022). URL <https://www.mdpi.com/2220-9964/11/1/24>.
- [46] Krajzewicz, D., Behrisch, M., Wagner, P., Luz, R. & Krumnow, M. Second generation of pollutant emission models for sumo. In Behrisch, M. & Weber, M. (eds.) *Modeling Mobility with Open Data*, 203–221 (Springer International Publishing, Cham, 2015).

- [47] Zhu, L., Holden, J. R. & Gonder, J. D. Trajectory segmentation map-matching approach for large-scale, high-resolution gps data. *Transportation Research Record* **2645**, 67–75 (2017). URL <https://doi.org/10.3141/2645-08>. <https://doi.org/10.3141/2645-08>.
- [48] Zhu, S. & Levinson, D. Do people use the shortest path? an empirical test of wardrop’s first principle. *PLOS ONE* **10**, 1–18 (2015). URL <https://doi.org/10.1371/journal.pone.0134322>.
- [49] Bazzani, A. *et al.* Towards congestion detection in transportation networks using gps data. In *2011 IEEE Third International Conference on Privacy, Security, Risk and Trust and 2011 IEEE Third International Conference on Social Computing*, 1455–1459 (IEEE, 2011).
- [50] Pappalardo, L. *et al.* Returners and explorers dichotomy in human mobility. *Nature Communications* **6**, 8166 (2015).
- [51] Zheng, Y. Trajectory data mining: An overview. *ACM Trans. Intell. Syst. Technol.* **6** (2015). URL <https://doi.org/10.1145/2743025>.